

Topological bands in two-dimensional networks of metamaterial elements

Vassilios Yannopoulos*

*Department of Materials Science, School of Natural Sciences,
University of Patras, GR-26504 Patras, Greece*

(Dated: October 8, 2018)

Abstract

We show that topological frequency band structures emerge in two-dimensional electromagnetic lattices of metamaterial components without the application of an external magnetic field. The topological nature of the band structure manifests itself by the occurrence of exceptional points in the band structure or by the emergence of one-way guided modes. Based on an EM network with nearly flat frequency bands of nontrivial topology, we propose a coupled-cavity lattice made of superconducting transmission lines and cavity QED components which is described by the Janes-Cummings-Hubbard model and can serve as simulator of the fractional quantum Hall effect.

PACS numbers: 42.70.Qs, 73.20.-r, 73.43.-f

I. INTRODUCTION

The topological description of the quantum states of matter sets in a new paradigm in the description and classification of atomic solids. Namely, atomic solids whose energy band structure possess nontrivial topological properties constitute a new class of materials whose salient properties are robust to phase transitions which modify the symmetry order of the atomic solid. Prominent examples of such topological atomic solids are the integer/fractional quantum Hall (I/FQHE) systems and the topological insulators (TIs). Well-known examples of topological properties are the existence of chiral edge states in QHE systems and the presence of gapless surface states in TIs which are both immune to order-disorder phase transitions.

The advent of artificial electromagnetic (EM) structures such as photonic crystals and metamaterials has established over the years a continuous conveyance of ideas and methods from atomic solids to their EM counterparts. Quite naturally, the concept of topological order has been adapted to photonic crystals starting with the QHE: a two-dimensional (2D) lattice of gyromagnetic/ gyroelectric cylinders is a system with broken time-reversal symmetry¹ with frequency bands characterized by a nonzero Chern number, allowing for the emergence of unidirectional (one-way) edge states² in analogy with the chiral edges states in QHE systems such as a 2D electron gas or graphene nanoribbons under magnetic field. Anomalous QHE can also be simulated with artificial chiral metamaterials of gyromagnetic components.³ In TIs⁴ and quantum spin Hall systems⁵ in 2D, the presence of magnetic field is not prerequisite for the appearance of topological electron states. In analogy with atomic TIs, in certain 3D photonic crystals and metamaterials with proper design, topological frequency bands appear without comprising gyromagnetic/ gyroelectric materials which require the application of external magnetic field in order to break time-reversal symmetry.⁶⁻⁸

In this Letter, we propose a class of 2D EM networks possessing topological frequency bands without the application of an external magnetic field. Namely, we show that topological bands emerge in 2D lattices of EM resonators connected with left- and right-handed metamaterial elements such as transmission lines or waveguides loaded with a negative refractive-index medium. The topological nature of the corresponding frequency bands is manifested by the emergence of an exceptional point for transverse electric (TE) and by the generation of one-way modes for transverse magnetic (TM) waves. In the latter case, the

system can be viewed as a simulator of the FQHE for polaritons.

II. LATTICE OF COUPLED DIPOLES.

The EM crystals under study here are amenable to a photonic tight-binding description within the framework of the coupled-dipole method.⁹ The latter is an exact means of solving Maxwell's equations in the presence of nonmagnetic scatterers. We consider a lattice of cavities within a lossless metallic host. The i -th cavity is represented by a dipole of moment $\mathbf{P}_i = (P_{i;x}, P_{i;y}, P_{i;z})$ which stems from an incident electric field \mathbf{E}^{inc} and the field which is scattered by all the other cavities of the lattice. This way the dipole moments of all the cavities are coupled to each other and to the external field leading to the coupled-dipole equation

$$\mathbf{P}_i = \alpha_i(\omega)[\mathbf{E}^{inc} + \sum_{i' \neq i} \mathbf{G}_{ii'}(\omega)\mathbf{P}_{i'}]. \quad (1)$$

$\mathbf{G}_{ii'}(\omega)$ is the electric part of the free-space Green's tensor and $\alpha_i(\omega)$ is the polarizability of the i -th cavity. Eq. (1) is a $3N \times 3N$ linear system of equations where N is the number of cavities of the system.

For a particle/cavity of electric permittivity ϵ embedded within a material host of permittivity ϵ_h , the polarizability α is provided by the Clausius-Mossotti formula $\alpha = (3V/4\pi)(\epsilon - \epsilon_h)/(\epsilon + 2\epsilon_h)$, where V is the volume of the particle/ cavity. For a lossless Drude-type (metallic) host i.e., $\epsilon_h(\omega) = 1 - \omega_p^2/\omega^2$ (where ω_p is the bulk plasma frequency), the polarizability α exhibits a pole at $\omega_0 = \omega_p \sqrt{2/(\epsilon + 2)}$ (surface plasmon resonance). By making a Laurent expansion of α around ω_0 and keeping the leading term,⁸ we may write $\alpha = F/(\omega - \omega_0) \equiv F/\Omega$ where $F = (27V/8\pi)\omega_0\epsilon/(2\epsilon + 4)$. For sufficiently high value of the permittivity of the dielectric cavity the electric field of the surface plasmon is much localized at the surface of the cavity. As a result, in a periodic lattice of cavities, the interaction of neighboring surface plasmons is very weak leading to much narrow frequency bands. By treating such a lattice in a tight binding (TB) manner,⁸ we may assume that the Green's tensor $\mathbf{G}_{ii'}(\omega)$ does not vary much with frequency and therefore, $\mathbf{G}_{ii'}(\omega) \simeq \mathbf{G}_{ii'}(\omega_0)$. In this case, Eq. (1) becomes an eigenvalue problem

$$\sum_{i' \neq i} \mathbf{G}_{ii'}(\omega_0)\mathbf{P}_{i'} = \Omega\mathbf{P}_i. \quad (2)$$

where F has been absorbed within the definition of $\mathbf{G}_{ii'}(\omega_0)$ and we have set $\mathbf{E}^{inc} = \mathbf{0}$ in Eq. (1) as we are seeking the eigenmodes of the system of cavities. In the following, we will be dealing with 2D lattices of cavities. We can, therefore, treat separately the case where the electric field lies within the plane of cavities (TE modes) from the case where the electric field is perpendicular to the plane (TM modes).

A. TE modes

In this case, $\mathbf{P}_i = (P_{i;x}, P_{i;y})$ and the Green's tensor $\mathbf{G}_{ii'}(\omega_0)$ is given by

$$\mathbf{G}_{ii'}(\omega_0) = Fq_0^3 \left[C(q_0|r_{ii'}|)\mathbf{I}_2 + J(q_0|r_{ii'}|) \begin{pmatrix} \frac{x_{ii'}^2}{r_{ii'}^2} & \frac{x_{ii'}y_{ii'}}{r_{ii'}^2} \\ \frac{x_{ii'}y_{ii'}}{r_{ii'}^2} & \frac{y_{ii'}^2}{r_{ii'}^2} \end{pmatrix} \right]. \quad (3)$$

with $\mathbf{r}_{ii'} = \mathbf{r}_i - \mathbf{r}_{i'}$, $q_0 = \omega_0 \sqrt{\epsilon_h(\omega_0)}/c$ and \mathbf{I}_2 is the 2×2 unit matrix. Since we focus our attention around the surface plasmon frequency ω_0 , we operate in the subwavelength regime where $q_0|r_{ii'}| \ll 1$. In this regime, the functions $C(q_0|r_{ii'}|)$, $J(q_0|r_{ii'}|)$ are written as

$$\begin{aligned} q_0^2 FC(q_0|r_{ii'}|) &\simeq -q_0^3 FJ(q_0|r_{ii'}|) \simeq q_0^3 F \exp(iq_0|r_{ii'}|)/(q_0|r_{ii'}|) \\ &= t_{ii'} \exp(i\phi_{ii'}) \end{aligned} \quad (4)$$

where $t_{ii'}$ and $\phi_{ii'}$ are real numbers. In what follows, the cavities are connected via coupling elements, i.e., waveguides or transmission lines, in which case the phase factors ϕ_{ij} are not necessarily related with the wavevector of the host medium ϵ_h and can therefore be considered as independent parameters.

For a 2D lattice of cavities, we assume the Bloch ansatz for the polarization field, i.e.,

$$\mathbf{P}_i = \mathbf{P}_{n\beta} = \exp(i\mathbf{k} \cdot \mathbf{R}_n)\mathbf{P}_{0\beta} \quad (5)$$

The cavity index i becomes composite, $i \equiv n\beta$, where n enumerates the unit cell and β the positions of inequivalent cavities in the unit cell. Also, \mathbf{R}_n denotes the lattice vectors and $\mathbf{k} = (k_x, k_y)$ is the Bloch wavevector. By substituting Eq. (5) into Eq. (2) we finally obtain

$$\sum_{\beta'} \tilde{\mathbf{G}}_{\beta\beta'}(\omega_0, \mathbf{k})\mathbf{P}_{0\beta'} = \Omega\mathbf{P}_{0\beta} \quad (6)$$

where

$$\tilde{\mathbf{G}}_{\beta\beta'}(\omega_0, \mathbf{k}) = \sum_{n'} \exp[i\mathbf{k} \cdot (\mathbf{R}_n - \mathbf{R}_{n'})] \mathbf{G}_{n\beta;n'\beta'}(\omega_0). \quad (7)$$

Solution of Eq. (6) provides the TE frequency band structure of a periodic system of cavities.

In order to seek for topological Bloch modes in a 2D lattice, we need at least two distinct frequency bands. Since, TE modes correspond to two degrees of freedom for the polarization field, i.e., (P_x, P_y) we may consider a 2D lattice with one cavity per unit cell. Namely, we consider the square lattice of Fig. 1a where we consider nearest-neighbor (NN) and next-nearest-neighbor (NNN) hoppings of the EM field among the cavities. The NN hopping carries a nonzero phase $t \exp(\pm\phi)$ whose signs are denoted by the arrows in Fig. 1a. The NNN hopping is denoted by t' . For the lattice of Fig. 1a, the Green's tensor $\tilde{\mathbf{G}}$ of Eq. (7) becomes

$$\begin{aligned} \tilde{\mathbf{G}} = & t[\cos\phi \cos(k_x\alpha/2) \cos(k_y\alpha/2) - i \sin\phi \sin(k_x\alpha/2) \sin(k_y\alpha/2)] \begin{pmatrix} 3 & -1 \\ -1 & 3 \end{pmatrix} \\ & + 2t' \begin{pmatrix} \cos(k_y\alpha) & 0 \\ 0 & \cos(k_x\alpha) \end{pmatrix} \end{aligned} \quad (8)$$

Fig. 1b shows the frequency band structure derived from Eq. (8) for $t = t' = 1$, $\phi = \pi/3$. We observe that at some point along the \overline{XM} symmetry line the frequency bands coalesce into a single band. The point beyond which the bands coalesce is an exceptional point and has been observed in \mathcal{PT} -symmetric lattices.¹⁰ In general, exceptional points emerging in parameter space are associated with topological charge and geometric (Berry) phase.¹¹ The topological properties of an exceptional point have been revealed by encircling it in parameter space¹² as it was demonstrated in a microwave cavity experiment.¹³ Although a proper theory of the topological properties of the exceptional points in lattices is still lacking, based on previous work¹¹ we can indirectly assign topological charge and geometric phase to the exceptional point appearing in the frequency band structure of Fig. 1b.

B. TM modes

Next, we assume that the polarization at each dipole is oriented in the z -axis. In this case, the eigenvalue problem of Eq. (2) becomes scalar and

$$G_{ii'} = Fq_0^3 C(q_{\parallel}|r_{ii'}|) \simeq q_0^3 F \exp(iq_0|r_{ii'}|)/(q_0|r_{ii'}|) = t_{ii'} \exp(i\phi_{ii'}). \quad (9)$$

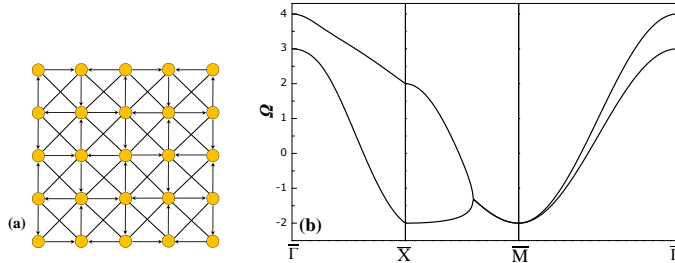


FIG. 1: (Color online) (a) Square lattice of EM resonators connected with metamaterial-based coupling elements. The arrows denote nearest-neighbor hoppings whilst the solid lines next-nearest-neighbor hoppings. The direction of the arrow shows whether wave propagation in the coupling element is left- or right-handed. (b) Frequency band structure corresponding to lattice of the left panel for $t = t' = 1$, $\phi = \pi/3$.

The same applies to Eqs. (6)-(7) and the TM problem becomes equivalent to the electronic case. Since the minimal model to have topological frequency bands is a two-band model, we adopt the checkerboard lattice of Ref. 14 (see Fig. 2a). Namely, apart from considering NN and NNN hoppings as in Fig. 1a, we also consider next-next-nearest-neighbor (NNNN) hoppings (denoted by the arcs in Fig. 2a) with strength t'' . The NN hoppings are, again, complex, $t \exp(\pm\phi)$ where the sign is denoted by the arrows in Fig. 2a. The NNN hopping strength is t'_1 (t'_2) if two sites are connected by a solid (dashed) line. We note that in EM lattices such as those considered here, a negative phase $-\phi$ can be easily achieved when the cavities are connected e.g., by 1D left-handed transmission lines (LHTL), i.e. transmission lines supporting backward-propagating waves where the phase velocity is opposite to the group velocity.^{15,16} Alternatively, the cavities may be connected by waveguides loaded with a left-handed (LH) metamaterial. Obviously, a positive phase $+\phi$ can be achieved by similar means [right-handed transmission lines (RHTLs)].

For the checkerboard lattice of Fig. 2a, the Green's tensor $\tilde{\mathbf{G}}_{\beta\beta'}$ becomes

$$\tilde{\mathbf{G}} = \begin{pmatrix} G_{11} & G_{12} \\ G_{21} & G_{22} \end{pmatrix} \quad (10)$$

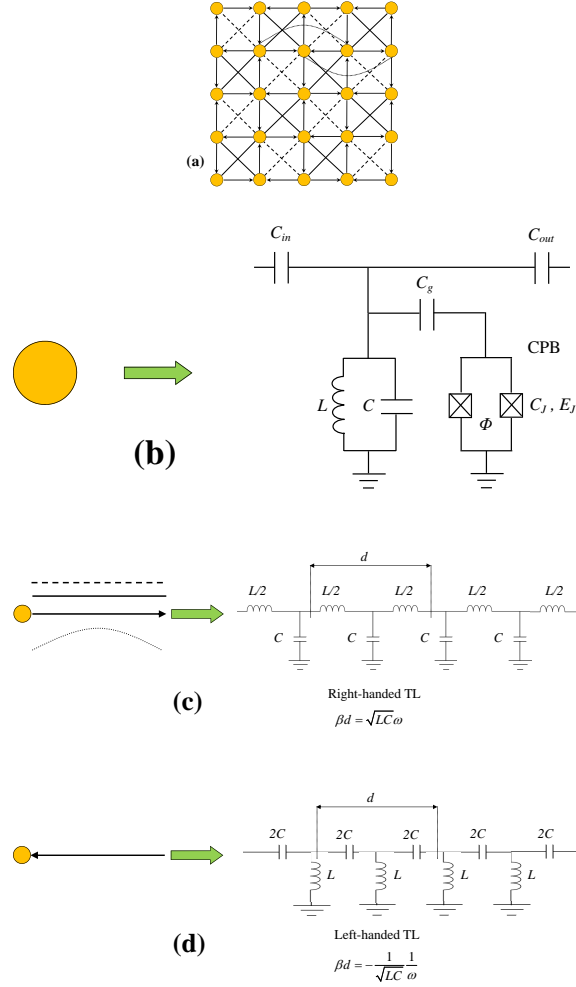


FIG. 2: (Color online) (a) Checkerboard lattice of EM resonators connected with metamaterial-based coupling elements. The arrows denote nearest-neighbor hoppings whilst the solid and broken lines next-nearest-neighbor hoppings. The direction of the arrow shows whether wave propagation in the coupling element is left- or right-handed. Two of the next-next-nearest neighbor hoppings are shown as dotted arcs. (b) The EM resonator of the lattice is a superconducting circuit QED system consisting of an LC resonator coupled to Cooper pair box (CPB). Typical transmission line for (c) right- ((d) left-) handed coupling elements along with the corresponding dispersion relation.

where

$$\begin{aligned}
 G_{11} &= 2t'_1 \cos(k_x \alpha) + 2t'_2 \cos(k_y \alpha) + 4t'' \cos(k_x \alpha) \cos(k_y \alpha) \\
 G_{12} = G_{21}^* &= 4t \cos \phi \cos(k_x \alpha / 2) \cos(k_y \alpha / 2) - 4it \sin \phi \sin(k_x \alpha / 2) \\
 G_{22} &= 2t'_2 \cos(k_x \alpha) + 2t'_1 \cos(k_y \alpha) + 4t'' \cos(k_x \alpha) \cos(k_y \alpha)
 \end{aligned} \tag{11}$$

Atomic lattices with exotic hoppings such as those considered here have been used for simulating fractional Quantum Hall effect (FQHE) states at zero magnetic field as nearly flat topological bands can emerge which simulate the Landau levels associated with a uniform magnetic field.¹⁷⁻¹⁹ By taking as TB parameters,¹⁴ $t = 1$, $\phi = \pi/4$, $t'_1 = -t'_2 = 1/(2 + \sqrt{2})$, $t'' = 1/(2 + 2\sqrt{2})$, a nearly flat band emerges as it is evident from the frequency band structure of Fig. 3a. Based on the equivalence of the Green's tensor of Eqs. (10) and (11) with the Hamiltonian of the electronic problem,¹⁴ each of the two bands of Fig. 3a carries a Chern number ± 1 . The topological nature of the frequency bands of the lattice of Fig. 2a is also manifested by the emergence of one-way bands (the photonic counterpart of the electron chiral edge states^{1,2}) in the frequency band structure for a slab geometry of Fig. 3b.

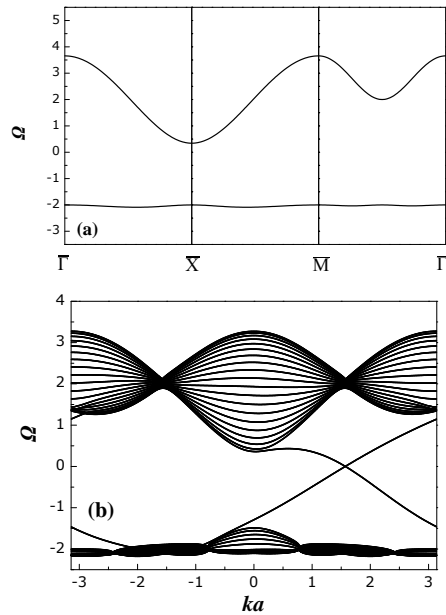


FIG. 3: (a) Frequency band structure for the infinite checkerboard lattice of Fig. 2 and (b) the frequency band structure for a finite slab consisting 20 unit planes [parameters: $t = 1$, $\phi = \pi/4$, $t'_1 = -t'_2 = 1/(2 + \sqrt{2})$, $t'' = 1/(2 + 2\sqrt{2})$]

The occurrence of topological properties such as the exceptional point in Fig. 1b and the one-way modes in Fig. 3 are a result the synthetic gauge field which is generated by the geometry of the metamaterial-based coupling elements (formation of closed flux loops of the phase of the EM field).

III. SIMULATION OF THE FQHE

Having established a nearly flat topological frequency band of the EM field for the lattice of Fig. 2a, we are able to design a system for creating an EM analog of the FQHE. The most natural choice would be to consider a coupled cavity array (CCW) wherein polaritons propagate through a hopping mechanism (as in our case) and interact strongly with the reservoir of modes when they reside within the cavity.^{20,21} FQHE with magnetic field can also be simulated by atoms confined in a 2D CCW.²² As stated above, the EM lattice of Fig. 2a can be realized in the laboratory as a network of transmission lines (TLs) where hoppings with positive (negative) phase can be realized with RHTLs (LHTLs) as shown in Fig. 2c (Fig. 2d). This means that the topological bands lie in the GHz regime. Therefore, in order to simulate the FQHE for microwave photons we need to implement a cavity QED scheme in this regime. This can be achieved by considering a superconducting-circuit cavity QED system^{23,24} consisting of a Cooper-pair box (CPB) coupled to a TL resonator (see the equivalent circuit of Fig. 2b). The CPB operates as an artificial atom (two-level system)^{25,26} and couples to the microwave photons of a superconducting TL resonator which plays the role of an on-chip cavity reservoir. The microwave response of superconducting circuit cavity QED system is described by the Jaynes-Cummings Hamiltonian^{23,24}

$$\begin{aligned}
 H^{JC} = & \hbar\omega_r(a_i^\dagger a_i + 1/2) - \frac{1}{2}(E_{el}\sigma_x^i + E_J\sigma_z^i) \\
 & + \hbar g(a_i^\dagger \sigma_i^- + a_i \sigma_i^+)
 \end{aligned}
 \tag{12}$$

where $\omega_r = 1/\sqrt{LC}$ is the frequency of the superconducting resonator, a_i^\dagger (a_i) creates (annihilates) a microwave photon in the TL resonator (cavity), σ_i^+ (σ_i) creates (annihilates) an excitation in the CPB, g is the coupling parameter between the CPB and the TL resonator, E_{el} is the electrostatic energy and $E_J = E_{J,max} \cos(\pi\Phi_b)$ the Josephson energy of the CPB. $\Phi_b = \Phi/\Phi_0$ is a flux bias applied by a coil to the CPB and controls the Josephson energy E_J .

A superconducting circuit cavity QED system where microwave photons propagate in the lattice of Fig. 2a is described by a Jaynes-Cummings-Hubbard Hamiltonian of the form²⁷

$$H^{JCH} = \sum_i H_i^{JC} + H^{TB}
 \tag{13}$$

where H^{TB} is the tight-binding form of the Hamiltonian of the microwave photons propa-

gating within the checkerboard lattice of Fig. 2a, i.e.,

$$\begin{aligned}
H^{TB} = & -t \sum_{\langle i,j \rangle} \exp(i\phi_{ij})(a_i^\dagger a_j + H.c.) - \sum_{\langle\langle i,j \rangle\rangle} t'_{ij}(a_i^\dagger a_j + H.c.) \\
& - t'' \sum_{\langle\langle\langle i,j \rangle\rangle\rangle} (a_i^\dagger a_j + H.c.)
\end{aligned} \tag{14}$$

which is the direct-space representation of the Green's tensor of Eq. (10). An important ingredient which gives rise to the FQHE is the presence of repulsive interactions among the microwave photons and is inherently present in Eq. (13) as photon blockade.²⁷ The latter phenomenon has been recently observed experimentally in the GHz regime for superconducting circuit cavity QED systems such as the one considered here (CPB + TL resonator).^{28,29} The different FQHE phases can be calculated by direct-diagonalization of the Hamiltonian of Eq. (13). We note that the proposed quantum simulator for the FQHE differs fundamentally with previous proposals^{30,31} since it essentially constitutes a passive design requiring no externally applied electric or magnetic fields.

Some typical values of the Hamiltonian of Eq. (13) are:²³ $\omega_r = 38$ GHz, $E_{J,max} = 8GHz$, $E_C = 5.2GHz$, $g \approx 0.314$ GHz. The latter parameter, g , is much larger than the loss rate of the TL resonator (~ 0.005 GHz) and the decoherence rate of the CPB (~ 0.004 GHz). The frequency ω_r of the TL resonator should fall within the operating bandwidth of the LH- and RHTLs. In Fig. 2c and Fig. 2d we have considered ideal TL which have infinite bandwidth. However, actual LH- and RHTLs have very large bandwidth which is a distinctive feature of nonresonant metamaterials compared to the resonant ones.¹⁶ Lastly, if the superconducting QED chip has a thickness of 1mm, the coupling TLs (RH or LH) have 10mm length and the TL resonator covers an area of 30mm², for the given resonator frequency (38GHz), the hopping strength t is about 0.5GHz which is also significantly larger than both the TL loss and CPB decoherence rates.

In order to probe experimentally the FQHE with the proposed structure one needs to create the phase diagram of the spectrum gap between the FQHE ground-state manifold and the lowest excited states, as a function of the coupling parameters g for NN and NNN hopping when the latter lie in the photon blockade regime. Generally speaking, in the FQHE state the spectral gap assumes much larger values than in superfluid and solid phases.¹⁸ The frequencies of the ground and excited states (and thus their corresponding gaps) can be measured by microwave transmission experiments.

IV. CONCLUSION

In conclusion, we have shown that topological frequency bands emerge in 2D electromagnetic lattices of metamaterial components in the absence of an applied magnetic field. The topological nature of the corresponding band structures gives rise to significant phenomena such as one-way waveguiding and coalescence of EM modes. The above lattices can be the basis for realizing a simulator for the FQHE based on superconducting transmission lines and circuit cavity QED systems.

* Electronic address: vyannop@upatras.gr

¹ F. D. M. Haldane and S. Raghu, Phys. Rev. Lett. **100**, 013904 (2008); *ibid*, Phys. Rev. A **78**, 033834 (2008).

² Z. Wang, Y. D. Chong, J. D. Joannopoulos, and M. Soljačić, Phys. Rev. Lett. **100**, 013905 (2008); *ibid*, Nature (London) **461**, 772 (2009); Z. Yu, G. Veronis, Z. Wang, and S. Fan, Phys. Rev. Lett. **100**, 023902 (2008); H. Takeda and S. John, Phys. Rev. A **78**, 023804 (2008); D. Han, Y. Lai, J. Zi, Z. Q. Zhang, and C. T. Chan, Phys. Rev. Lett. **102**, 123904 (2009); X. Ao, Z. Lin, and C. T. Chan, Phys. Rev. B **80**, 033105 (2009); M. Onoda and T. Ochiai, Phys. Rev. Lett. **103**, 033903 (2009); T. Ochiai and M. Onoda, Phys. Rev. B **80**, 155103 (2009); R. Shen, L. B. Shao, B. Wang, and D. Y. Xing, Phys. Rev. B **81**, 041410(R) (2010); Y. Poo, R. X. Wu, Z. Lin, Y. Yang, and C. T. Chan, Phys. Rev. Lett. **106**, 093903 (2011).

³ V. Yannopoulos, Phys. Rev. B **83**, 113101 (2011).

⁴ L. Fu, C. L. Kane, and E. J. Mele, Phys. Rev. Lett. **98**, 106803 (2007); L. Fu and C. L. Kane, Phys. Rev. B **76**, 045302 (2007); M. Z. Hasan and C. L. Kane, Rev. Mod. Phys. **82**, 3045 (2010).

⁵ C. L. Kane and E. J. Mele, Phys. Rev. Lett. **95**, 226801 (2005); *ibid*, Phys. Rev. Lett. **95**, 146802 (2005).

⁶ W.-J. Chen, Z. H. Hang, J.-W. Dong, X. Xiao, H.-Z. Wang, and C. T. Chan, Phys. Rev. Lett. **107**, 023901 (2011).

⁷ W. Zhong and X. Zhang, Opt. Express **19**, 13738 (2011).

⁸ V. Yannopoulos, Phys. Rev. B **84**, 195126 (2011).

⁹ E. M. Purcell and C. R. Pennypacker, Astrophys. J. **186**, 705 (1973).

- ¹⁰ K. G. Makris, R. El-Ganainy, D. N. Christodoulides, and Z. H. Musslimani, Phys. Rev. Lett. **100**, 103904 (2008); S. Klaiman, U. Günther, and N. Moiseyev, Phys. Rev. Lett. **101**, 080402 (2008); S. Longhi, Phys. Rev. Lett. **103**, 123601 (2009); M. Botey, R. Herrero, and K. Staliunas, Phys. Rev. A **82**, 013828 (2010).
- ¹¹ U. Günther, I. Rotter, and B. F. Samsonov, J. Phys. A: Math. Theor. **40**, 8815 (2007); F. Keck, H. J. Korsch, and S. Mossman, J. Phys. A: Math. Gen. **36**, 2125 (2003); A. I. Nesterov and F. Aceves de la Cruz, J. Phys. A: Math. Theor. **41**, 485304 (2008).
- ¹² W. D. Hess, Eur. Phys. J. D **7**, 1 (1999).
- ¹³ C. Dembowski, H.- D. Gräf, H. L. Harney, A. Heine, W. D. Heiss, H. Rehfeld, and A. Richter, Phys. Rev. Lett. **86**, 787 (2001).
- ¹⁴ K. Sun, Z. Gu, H. Katsura, and S. Das Sarma, Phys. Rev. Lett. **106**, 236803 (2011).
- ¹⁵ A. K. Iyer and G. V. Eleftheriades, *Negative Refraction Metamaterials: Fundamental Principles and Applications*, edited by G. V. Eleftheriades and K. G. Balmain (Wiley-IEEE Press, New York, 2005) p. 1
- ¹⁶ C. Caloz and T. Itoh, *Electromagnetic Metamaterials: Transmission Line Theory and Microwave Applications* (Wiley-IEEE Press, New Jersey, 2006).
- ¹⁷ T. Neupert, L. Santos, C. Chamon, and C. Mudry, Phys. Rev. Lett. **106**, 236804 (2011).
- ¹⁸ Y.- F. Wang, Z.- C. Gu, C.- D. Gong, and D. N. Sheng, Phys. Rev. Lett. **107**, 146803 (2011).
- ¹⁹ D. N. Sheng, Z.- C. Gu, K. Sun, and L. Sheng, Nature Commun., DOI:10.1038/ncomms1380, (2011).
- ²⁰ A. D. Greentree, C. Tahan, J. H. Cole, and L. C. L. Hollenberg, Nature Phys. **2**, 856 (2006); M. J. Hartmann, F. G. S. L. Brandão, and M. B. Plenio, Nature Phys. **2**, 849 (2006); D. G. Angelakis, M. F. Santos, and S. Bose, Phys. Rev. A **76**, 031805 (2007); M. J. Hartmann, F. G. S. L. Brandão, and M. B. Plenio, Laser Photon. Rev. **2**, 527 (2008).
- ²¹ L. Zhou, Y. B. Gao, Z. Song, and C. P. Sun, Phys. Rev. A **77**, 013831 (2008).
- ²² J. Cho, D. G. Angelakis, and S. Bose, Phys. Rev. Lett. **101**, 246809 (2008).
- ²³ A. Wallraff, D. I. Schuster, A. Blais, L. Frunzio, R.- S. Huang, J. Majer, S. Kumar, S. M. Girvin, and R. J. Schoelkopf, Nature (London) **431**, 162 (2004).
- ²⁴ A. Blais, R.- S. Huang, A. Wallraff, S. M. Girvin, and R. J. Schoelkopf, Phys. Rev. A **69**, 062320 (2004).
- ²⁵ V. Bouchiat, D. Vion, P. Joyez, D. Esteve, and M. H. Devoret, Phys. Scripta **76**, 165 (1998).

- ²⁶ J. Clarke and F. K. Wilhelm, *Nature (London)* **453** 1031 (2008).
- ²⁷ M. I. Makin, J. H. Cole, C. Tahan, L. C. L. Hollenberg, and A. D. Greentree, *Phys. Rev. A* **77**, 053819 (2008).
- ²⁸ C. Lang, D. Bozyigit, C. Eichler, L. Steffen, J. M. Fink, A. A. Abdumalikov Jr., M. Baur, S. Filipp, M. P. da Silva, A. Blais, and A. Wallraff, *Phys. Rev. Lett.* **106**, 243601 (2011).
- ²⁹ A. J. Hoffman, S. J. Srinivasan, S. Schmidt, L. Spietz, J. Aumentado, H. E. Türeci, and A. A. Houck, *Phys. Rev. Lett.* **107**, 053602 (2011).
- ³⁰ J. Koch, A. A. Houck, K. L. Hur, and S. M. Girvin, *Phys. Rev. A* **82**, 043811 (2010); A. Nunnenkamp, J. Koch, and S. M. Girvin, *New J. Phys.* **13**, 095008 (2011).
- ³¹ M. Hafezi, E. A. Demler, M. D. Lukin, and J. M. Taylor, *Nature Phys.* **7**, 907 (2011).